Experimental Hematology

Experimental Hematology 2019;70:55–69

Deferasirox selectively induces cell death in the clinically relevant population of leukemic CD34$^+$CD38$^-$ cells through iron chelation, induction of ROS, and inhibition of HIF1α expression

Saar Shapira[a,b], Pia Raanani[b,c], Aladin Samara[a,b], Arnon Nagler[b,d], Ido Lubin[a,b], Nadir Arber[b,e], and Galit Granot[a]

[a]*Felsenstein Medical Research Center, Beilinson Hospital, Rabin Medical Center, Petah-Tikva, Israel;* [b]*Sackler School of Medicine, Tel Aviv University, Tel Aviv, Israel;* [c]*Institute of Hematology, Davidoff Cancer Center, Beilinson Hospital, Rabin Medical Center, Petah-Tikva, Israel;* [d]*Department of Hematology and Bone Marrow Transplantation, Chaim Sheba Medical Center, Tel-Hashomer, Ramat-Gan, Israel;* [e]*Integrated Cancer Prevention Center and Department of Gastroenterology, Tel Aviv Sourasky Medical Center, Tel Aviv, Israel*

(Received 24 April 2018; revised 21 October 2018; accepted 30 October 2018)

Despite a high remission rate after therapy, only 40–50% of acute myeloid leukemia (AML) patients survive 5 years after diagnosis. The main cause of treatment failure is thought to be insufficient eradication of CD34$^+$CD38$^-$ AML cells. In order to induce preferential cell death in CD34$^+$CD38$^-$ AML cells, two separate events may be necessary: (1) inhibition of survival signals such as nuclear factor kappa-beta (NF-κB) and (2) induction of stress responses such as the oxidative stress response. Therefore, regimens that mediate both effects may be favorable. Deferasirox is a rationally designed oral iron chelator mainly used to reduce chronic iron overload in patients who receive long-term blood transfusions. Our study revealed that clinically relevant concentrations of deferasirox are cytotoxic in vitro to AML progenitor cells, but even more potent against the more primitive CD34$^+$CD38$^-$ cell population. In addition, we found that deferasirox exerts its effect, at least in part, by inhibiting the NF-κB/hypoxia-induced factor 1-alpha (HIF1α) pathway and by elevating reactive oxygen species levels. We believe that, pending further characterization, deferasirox can be considered as a potential therapeutic agent for eradicating CD34$^+$CD38$^-$ AML cells.

Acute myelogenous leukemia (AML) is a clonal malignancy that is thought to be initiated at a stage as early as hematopoietic stem/progenitor cells [1]. The cure rates are less than 10% for older AML patients and the median survival is less than 1 year for these patients [2]. Although 70–80% of younger patients achieve complete remission, most will eventually relapse and overall survival is only 40–50% at 5 years [3,4]. Drug resistance and relapse are major causes for treatment failure. Current treatments for AML such as nucleoside analogs (e.g., cytosine arabinoside [ARA-C]) and anthracyclines [e.g., idarubicin, daunorubicin]) interfere with DNA replication and induce apoptosis primarily in replicating cells [4,5]. Because AML CD34$^+$CD38$^-$cells are mostly quiescent [6] and maintain drug resistance capabilities [7], it is likely that at least some of these cells are refractory to these treatments and may thereby contribute to relapse [8–11].

It has been shown that AML patients with a greater number of CD34$^+$CD38$^-$ cells at diagnosis have inferior clinical outcomes compared with those who had fewer CD34$^+$CD38$^-$ cells [12–15]. A different study showed that CD34$^+$CD38$^-$ cells are only minimally affected by conventional chemotherapy and minimal residual disease (MRD) was found to be enriched with these cells [16]. Due to the likelihood that the MRD population contains CD34$^+$CD38$^-$ cells [17–19], it is reasonable to assume that treatment regimens that function by eliminating CD34$^+$CD38$^-$ cells will reduce MRD and improve outcome for AML patients. Therefore, identifying the "Achilles heel" of CD34$^+$CD38$^-$ cells and determining how they differ from normal hematopoietic stem cells is required for the

Offprint requests to: Dr. Galit Granot, Ph.D., Felsenstein Medical Research Center, Rabin Medical Center, Israel; E-mail: galitg@clalit.org.il

Supplementary material associated with this article can be found, in the online version, at doi:10.1016/j.exphem.2018.08.003.

0301-472X/
https://doi.org/10.1016/j.exphem.2018.10.010

development of effective targeted and curative therapies. These data also imply that the $CD34^+CD38^-$ cell fraction is a clinically relevant fraction in the propagation of AML and may hold a key role in the mechanism of relapsed AML and that eliminating this therapy-resistant fraction represents a possible path toward achieving longer remissions.

Identifying the molecular mechanisms that underlie the enhanced survival and drug resistance qualities of $CD34^+CD38^-$ cells is critical for targeting this difficult to eradicate population [20,21]. Nuclear factor kappa-beta (NF-κB) is activated in the more primitive leukemic cells of AML, but not in normal hematopoietic stem cells [9,22,23], and NF-κB-associated pathways are thus known to be related to tumor formation and maintenance [24]. Therefore, finding agents that inhibit NF-κB may represent a beneficial approach to more durable AML therapy. Indeed, inhibition of NF-κB signaling via parthenolide derivatives [10], proteasome inhibitors [25], and direct inhibition of inhibitor of NF-κB kinase [26] has been shown to induce apoptosis in AML blasts. In addition, NF-κB regulates the expression of the hypoxia-induced factor 1-alpha (HIF1α) transcription factor [27]. Recent studies have shown that HIF1α plays a key role in the maintenance of chronic myeloid leukemia-initiating cells and targeting HIF1α eliminates cancer stem cells in hematological malignancies [28,29]. However, data have shown that the sole inhibition of NF-κB is not sufficient to induce adequate $CD34^+CD38^-$-specific apoptosis [25,26].

Studies have demonstrated that increased oxidative load is a prevalent component of the AML cell death process and that primitive AML cells may be more sensitive to changes in oxidative state than the more mature leukemic blasts [10]. Collectively, these data suggest that two separate events may be necessary to induce preferential cell death in primitive leukemic cells: (1) inhibition of survival signals such as NF-κB and (2) induction of stress responses such as the oxidative stress response. Therefore, regimens that mediate both effects may be favorable. Deferasirox is a rationally designed oral iron chelator mainly used to reduce chronic iron overload in patients who receive long-term blood transfusions [30]. It is also a powerful NF-κB inhibitor in myelodysplastic cells and in leukemia cell lines [31]. Additionally, deferasirox has been shown to induce reactive oxygen species (ROS) generation in hematopoietic stem cells, myelodysplastic hematopoietic progenitor cells, and other leukemic cell lines [32–34].

To date, the effect of deferasirox on $CD34^+CD38^-$ cells has not been examined. This work shows that clinically relevant concentrations of deferasirox decreased $CD34^+CD38^-$ cell viability via the induction of apoptosis and inhibition of proliferation. Apoptosis induction was associated with an elevation in ROS levels, inhibition of NF-κB translocation to the nucleus, and the subsequent downregulation of HIF1α, a known key factor in $CD34^+CD38^-$ cell maintenance.

Methods

Cell isolation and culture

Primary AML cells were obtained, with written informed consent, from bone marrow of newly diagnosed patients at the Division of Hematology, Davidoff Center, Rabin Medical Center, Israel, and at the Division of Hematology, Sheba Medical Center, Israel. This research was approved by the Rabin Medical Center and the Sheba Medical Center institutional review boards and ethics committees. The human AML cell line KG-1a (kindly provided by Prof. Tsvee Lapidot, Weizmann Institute of Science) was also used. For mononuclear cell and $CD34^+CD38^-$/$CD34^+CD38^+$ separations, see the Supplementary Methods (online only, available at www.exphem.org).

Apoptosis

Apoptosis was assessed using an Annexin V/phycoerythrin staining kit (Abcam, Cambridge, UK) according to the manufacturer's instructions and 7-amino-actinomycin D (7-AAD) staining (Thermo Fisher Scientific, Waltham, MA, USA). Analysis was performed on a Gallios flow cytometer and data were processed by Kaluza (Beckman Coulter, Indianapolis, IN, USA) software. The total number of events collected was 25,000.

Cell cycle

Cells (1×10^6) were fixed with 100% ice-cold methanol, washed with cold phosphate-buffered saline (PBS), and then stained with PBS containing 50 μg/mL propidium iodide (PI) (Sigma-Aldrich, Rehovot, Israel), 100 μg/mL RNase A (Sigma-Aldrich), and 0.1% Triton X-100 (Sigma-Aldrich). Samples were incubated in the dark for 30 minutes. Bromodeoxyuridine (BrdU) incorporation was measured using the fluorescein isothiocyanate (FITC) BrdU flow kit (BD Pharmingen, San Jose, CA, USA) according to the manufacturer's protocol. All analyses were measured by a Gallios flow cytometer. Data were analyzed using Kaluza software.

Colony-forming assay

Cells (1×10^4) were incubated at 37°C in complete methylcellulose medium with recombinant cytokines (MethoCult H4434; STEMCELL Technologies, Vancouver, Canada). Colonies were counted after 10 days with an inverted microscope (Olympus, Hamburg, Germany). Colonies were defined as clusters containing >20 cells. For representative enlarged images of the colonies, see the Supplementary Methods (online only, available at www.exphem.org).

Cell fractionations

Nuclear and cytoplasmic proteins were isolated using NE-PER nuclear and cytoplasmic extraction reagents (Thermo Fisher Scientific) according to the manufacturer's instructions. Fractionation efficiency was determined by Histon H4 (nuclear protein) and β-tubulin (cytoplasmic protein) antibodies.

Chromatin immunoprecipitation

Chromatin immunoprecipitation (ChIP) was performed with the Magna-CHIP chromatin immunoprecipitation kit (Millipore, Burlington, MA, USA) according to the manufacturer's instructions. For detailed methods, see the Supplementary Methods (online only, available at www.exphem.org).

Intracellular ROS measurement

Intracellular ROS levels were determined by 2′,7′-dichlorodihydrofluorescein-diacetate (H_2DCFDA) cellular ROS detection assay kit (Abcam). Detection of free thiol groups was performed using monochlorobimane (mBCl) staining. Mitochondrial ROS level was determined using the MitoSOXRed Mitochondrial Superoxide Indicator (Thermo Fisher Scientific). Detailed protocol is provided in the Supplementary Methods (online only, available at www.exphem.org).

Hypoxia induction

Sorted KG-1a cells were treated with relevant concentrations of deferasirox and immediately placed in a "hypoxia tank" (STEMCELL Technologies) containing a 1% O_2 gas mixture for 48 hours. Cells were then lysed and protein extracts were analyzed by Western blot.

Western blot

Proteins were separated on Mini-PROTEAN precast gels (Bio-Rad, Hercules, CA, USA), transferred to a nitrocellulose Trance-Blot Turbo Transfer Pack membrane (Bio-Rad), and then blotted with the antibodies listed in the Supplementary Methods (online only, available at www.exphem.org).

Small interfering RNA transfection

Cells were electroporated with small interfering RNAs (siRNAs) using the Amaxa Cell Line Nucleofector Kit L (Lonza, Basel, Switzerland) according to the manufacturer's protocol. Electroporation parameters were set according to the Amaxa Kit L protocol for KG-1a cells. Cells were analyzed 24 hours after transfection. HIF-1α siRNA sense was: 5′-CCUCAGUGUGGGUAUAAGAtt-3′; antisense was: 5′-UCUUAUACCCACACUGAGGtt-3′ (Applied Biosystems, Foster City, CA, USA).

Real-time polymerase chain reaction

RNA was isolated using the RNeasy Plus Mini Kit (Qiagen, Hilden, Germany) and reverse transcribed using the high-capacity cDNA RT kit (Applied Biosystems). Real-time polymerase chain reaction (PCR) was performed using the Eco Real-Time PCR (Illumina, San Diego, CA, USA). Amplification conditions are listed in the Supplementary Methods (online only, available at www.exphem.org).

Statistics

Unless differently indicated, Student t test was used. Statistical significance was given at $p < 0.05$. One-way analysis of variance (ANOVA) followed by Bonferroni's post hoc test and two-way ANOVA were performed using IBM SPSS 24 software. Synergism was calculated by Chou.T.C combination index using ComboSyn software (www.combosyn.com).

Results

Deferasirox selectively eradicates KG-1a $CD34^+CD38^-$ cells and exhibits a synergistic effect with ARA-C

Deferasirox inhibits NF-κB [31]. Given the critical role of NF-κB in $CD34^+CD38^-$ AML cells [9] and the key role of iron in hematopoietic stem cell cellular metabolism, we were intrigued by the possibility that AML $CD34^+CD38^-$ cells can be selectively targeted by deferasirox.

Because AML $CD34^+CD38^-$ cells are only minimally affected by conventional chemotherapy and MRD was found to be enriched within these cells, they are potentially clinically relevant [16]. We therefore used the $CD34^+CD38^-$ fraction for all experiments. $CD34^+CD38^-$ cells sorted from the KG-1a cell line have been shown to be morphologically, cytochemically, and functionally primitive. These cells also possess stem cell characteristics and were therefore chosen as model cells [35]. $CD34^+CD38^-$ KG-1a cells exhibited increased sensitivity to deferasirox with a half-maximal inhibitory concentration of 1.3 μmol/L compared with 8.9 μmol/L calculated for the more mature $CD34^+CD38^+$ cells (Figure 1A). The $CD34^+CD38^-$ KG-1a cells were less sensitive to ARA-C compared with $CD34^+CD38^+$ cells (Figure 1B). Combination index indicated a synergistic effect between deferasirox and ARA-C, most prominently with the lower doses of these two drugs both in the primitive and in the more mature populations (Figures 1C–1F).

Deferasirox induces growth arrest of the $CD34^+CD38^-$ KG-1a cells, the AML patient $CD34^+CD38^-CD123^+$ cell population, and the corresponding progenitor cells

Previous studies have shown that exposing lymphoma cell lines to deferasirox results in G_1/S arrest [36]. We therefore assessed whether the cytotoxic effect of deferasirox on the KG-1a cells was due to growth arrest. Cell fractions were cultured in 5 μmol/L or 20 μmol/L deferasirox, which are clinically relevant concentrations of the drug [37], or in the presence of dimethylsulfoxide (DMSO) as a control. Following 48 hours of exposure to 20 μmol/L deferasirox, a significant number of S-phase cells were detected both in the KG-1a $CD34^+CD38^-$ cells (control: 15±2.5%, 20 μmol/L deferasirox: 26.4 ± 2.2%, $p < 0.05$) and in the KG-1a $CD34^+CD38^+$ progenitor cells (control: 25.1± 2.3%, 20 μmol/L deferasirox: 32.6 ± 1.4%, $p < 0.05$) (Figure 2A). In a colony-forming assay, the number of colonies formed by both primitive and mature cell fractions was reduced following exposure to deferasirox in a dose-dependent manner (Figure 2B). Deferasirox also reduced the number of colonies formed by AML patients' $CD34^+CD38^-CD123^+$ fraction and progenitor

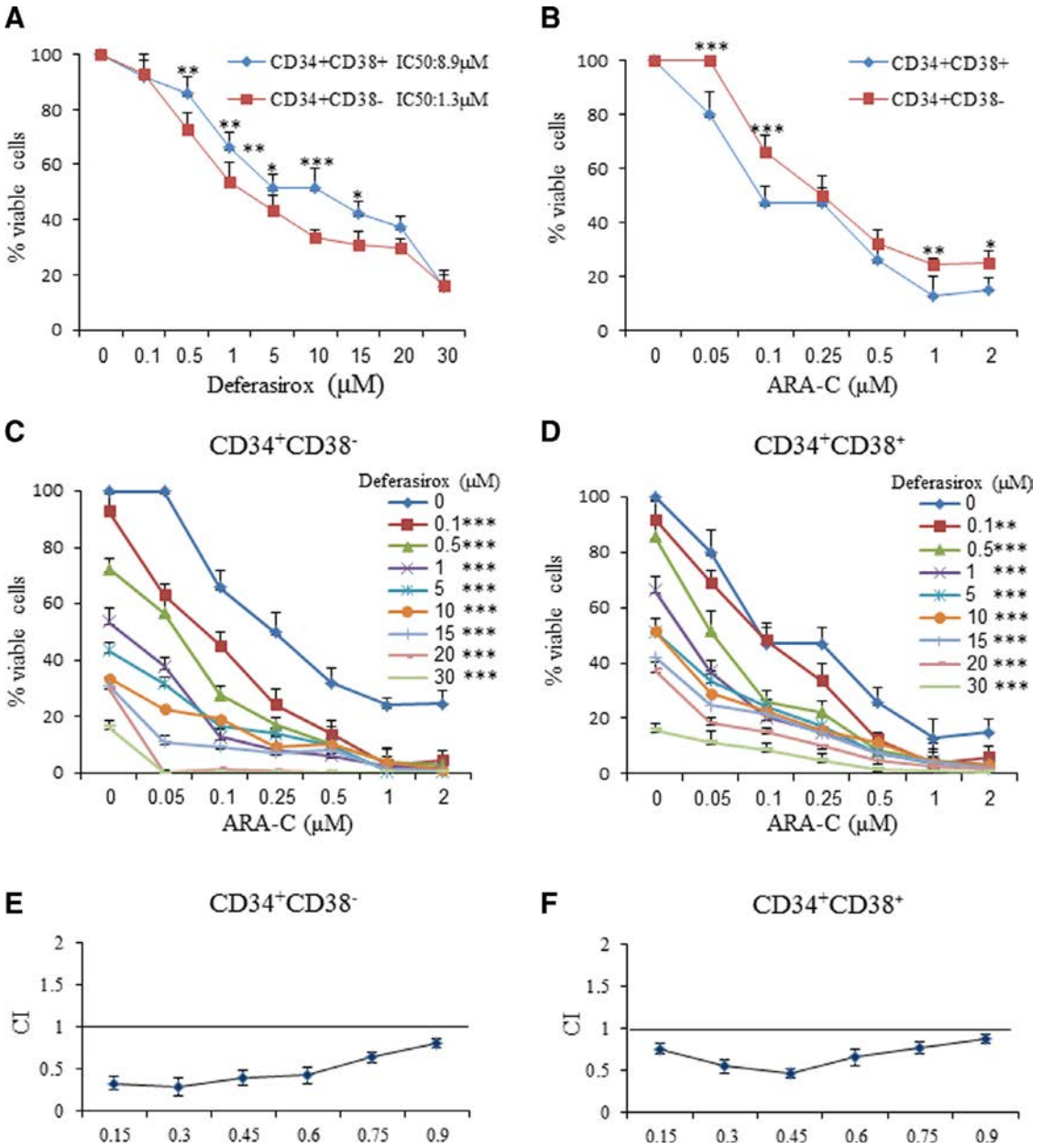

Figure 1. Deferasirox selectively eradicates KG-1a $CD34^+CD38^-$ cells. KG-1a $CD34^+CD38^-$ and $CD34^+CD38^+$ fractions were exposed to deferasirox **(A)** and ARA-C **(B)** separately and combined **(C,D)** for 72 hours. Values represent a mean of three experiments ± SD ($n = 3$). Two-way ANOVA was performed. Presented are simple main effects comparing each deferasirox concentration between the two cell types **(A,B)** and main effects comparing the overall effect of deferasirox on viability averaging across the different concentrations of ARA-C to the untreated control **(C,D)**. *$p < 0.05$, **$p < 0.01$, ***$p < 0.001$. Cell proliferation was analyzed by WST-1. Synergism was calculated by Chou.T.C combination index **(E,F)**.

cell fractions. The 20 μmol/L concentration reduced colony formation by over 93% in all groups ($p < 0.01$) (Figure 2B). The vast majority of the colonies appeared abnormal and exhibited blast-like or monocytic features with the exception of several granulocyte/macrophage colonies. In addition, we tracked cell division by staining KG-1a $CD34^+CD38^-$ and $CD34^+CD38^+$ cells with eFluor proliferation dye for 96 hours. As shown in Figure 2C, deferasirox inhibited cell division in both cell fractions. At a high deferasirox concentration (20 μmol/L), the percentage of nondividing $CD34^+CD38^-$ and $CD34^+CD38^+$ KG-1a cells was 71.8% and 66.2%, respectively, compared with the respective 6.9% and 10.2% in the untreated cells. Both the colony-forming assay and the proliferation dye experiment pointed to a substantial inhibition of proliferation by deferasirox. This inhibition cannot be explained by the mild S-phase arrest that was observed

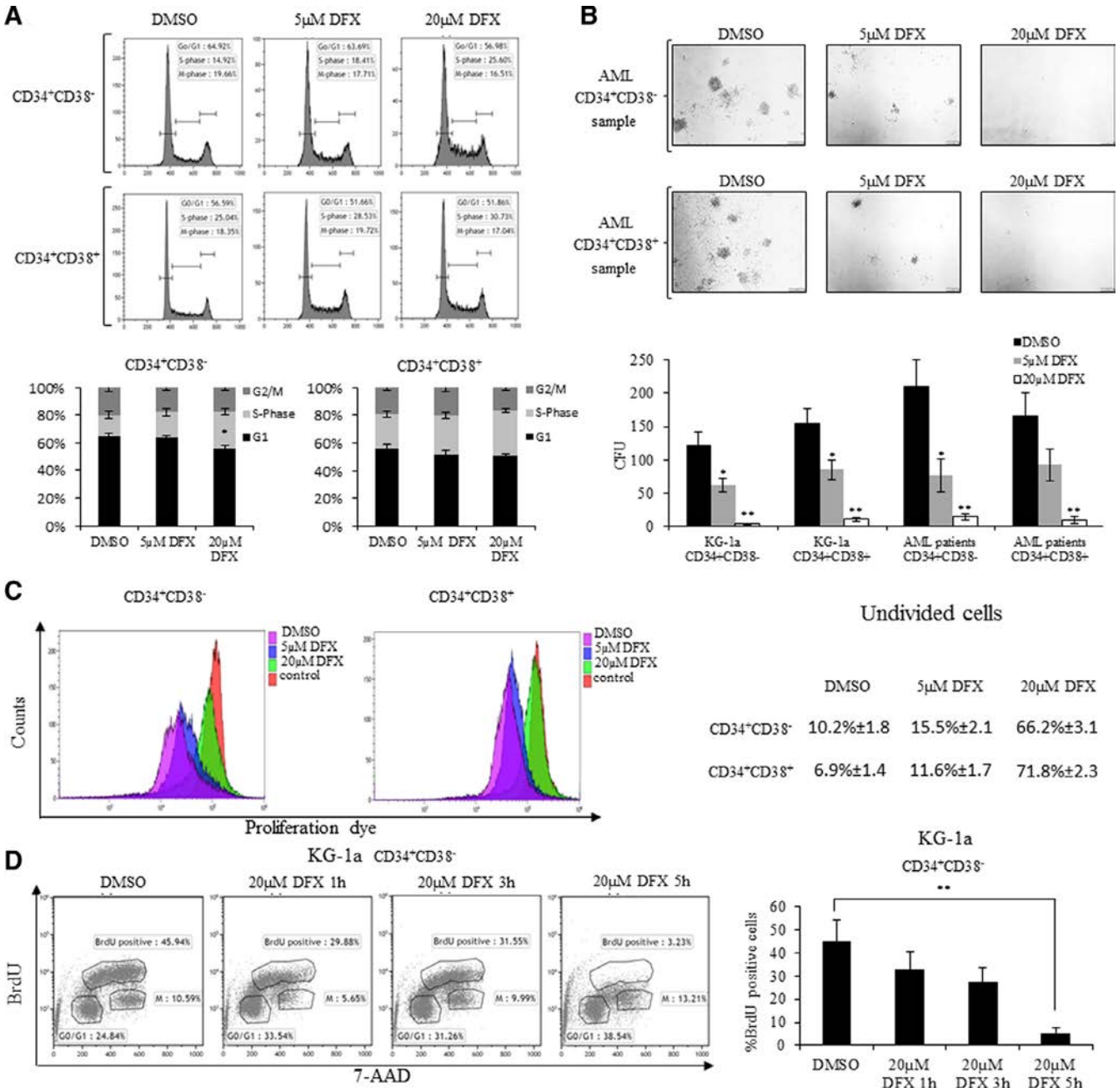

Figure 2. Deferasirox induces growth arrest. KG-1a cells were separated into $CD34^+CD38^-$ and $CD34^+CD38^+$ fractions **(A–D)**. $CD34^+CD38^-CD123^+$ and $CD34^+CD38^+CD123^+$ cells were isolated from newly diagnosed AML patients ($n = 3$) **(B).** **(A)** KG-1a $CD34^+CD38^-$ and $CD34^+CD38^+$ samples were cultured with 5 μmol/L and 20 μmol/L deferasirox for 48 hours. Cell cycle was evaluated by PI staining. Values represent a mean of three experiments ± SEM supplemented with histograms of one representative experiment. **(B)** Following a 48 hour incubation of KG-1a $CD34^+CD38^-$ and $CD34^+CD38^+$ cells and AML $CD34^+CD38^-CD123^+$ and $CD34^+CD38^+CD123^+$ cells with deferasirox, the cells were seeded in complete methylcellulose medium with recombinant cytokines for 10 days. Samples were screened for colonies using an inverted microscope. Values represent a mean of three experiments carried out on samples from three different patients (patient samples: AML11, AML15, and AML22) ± SEM accompanied by inverted microscope images from one representative experiment (AML15). $*p < 0.05$, $**p < 0.01$. CFU = colony-forming units. **(C)** KG-1a $CD34^+CD38^-$ and $CD34^+CD38^+$ fractions were staining with an eFluor proliferation dye, incubated for 96 hours, and analyzed by flow cytometry. Percentages of undivided cells are presented ± SEM ($n = 3$), supplemented by a histogram of one representative experiment. **(D)** $CD34^+CD38^-$ KG-1a cells were treated with 20 μmol/L deferasirox for 1, 3, and 5 hours and then the cells were pulsed with BrdU for 45 min followed by anti-BrdU FITC and 7-AAD staining and flow cytometry. The percentage of S-phase gated cells are presented, accompanied by dot plots from one representative experiment. Values represent a mean of three experiments ± SEM. $**p < 0.01$.

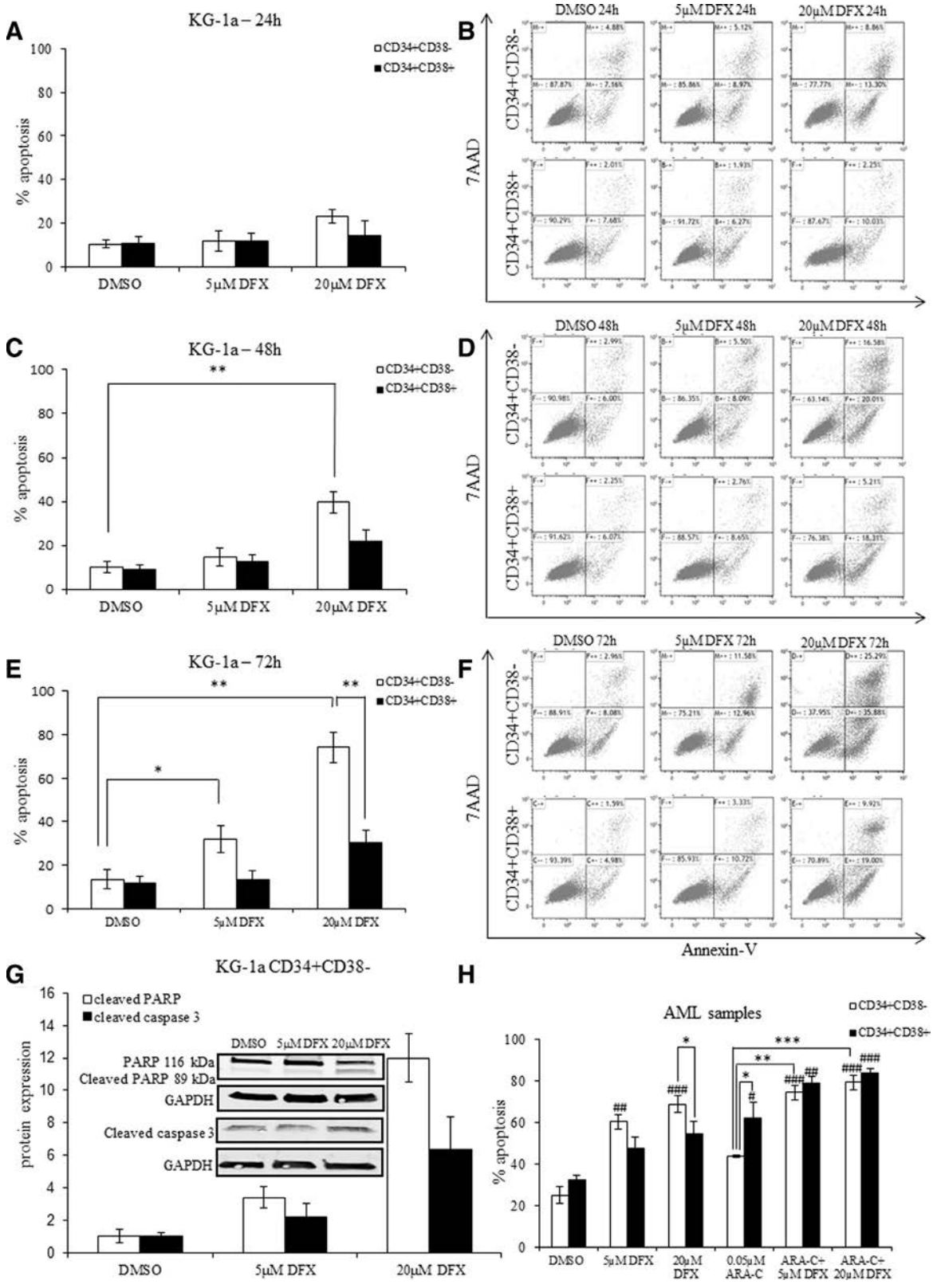
A
KG-1a – 24h
CD34+CD38-
CD34+CD38+
% apoptosis
DMSO
5μM DFX
20μM DFX
B
DMSO 24h
5μM DFX 24h
20μM DFX 24h
CD34+CD38-
CD34+CD38+
7AAD
C
KG-1a – 48h
D
DMSO 48h
5μM DFX 48h
20μM DFX 48h
E
KG-1a – 72h
F
DMSO 72h
5μM DFX 72h
20μM DFX 72h
Annexin-V
G
KG-1a CD34+CD38-
cleaved PARP
cleaved caspase 3
protein expression
PARP 116 kDa
Cleaved PARP 89 kDa
GAPDH
Cleaved caspase 3
H
AML samples
0.05μM ARA-C
ARA-C+ 5μM DFX
ARA-C+ 20μM DFX

following deferasirox treatment (Figure 2A). We therefore performed a more sensitive assay. We monitored DNA synthesis in deferasirox-treated KG-1a $CD34^+CD38^-$ cells using BrdU and 7-AAD staining (Figure 2D). Interestingly, even after a short 1 hour exposure to 20 μmol/L deferasirox, we observed a significant reduction in BrdU incorporation, suggesting a decrease in DNA transcription. Following 1, 3, and 5 hours of exposure to deferasirox, the S-phase-gated, BrdU-positive $CD34^+CD38^-$ KG-1a cells percentages decreased by 26 ± 7.5%, 39 ± 6.3%, and 88 ± 2.4%, respectively (Figure 2D). Together, these data suggest that deferasirox leads to a statistically significant reduction in the proliferation of the $CD34^+CD38^-$ and $CD34^+CD38^+$ KG-1a cell populations and in AML patient primary cells.

Deferasirox induces apoptosis in KG-1a $CD34^+CD38^-$ cells and in the AML patient $CD34^+CD38^-CD123^+$ cell population

We next examined the apoptotic effect of deferasirox on $CD34^+CD38^-$ and $CD34^+CD38^+$ KG1a cell fractions. To this end, the cell fractions were cultured in 5 μmol/L or 20 μmol/L deferasirox for 24–72 hours or in DMSO as control and stained with Annexin V and the plasma membrane permeability marker 7-AAD. Deferasirox showed a significant time- and dose-dependent induction of apoptosis in the $CD34^+CD38^-$ cells. The percent of apoptotic cells was 21.9 ± 2.8%, 39.7 ± 4.9%, and 73.95 ± 6.1% following a 24, 48, and 72 hour exposure to 20 μmol/L deferasirox and 32 ± 6.2% and 73.95 ± 6.1% following exposure to 5 μmol/L and 20 μmol/L deferasirox (72 hours), respectively (Figures 3A–3F). Our data show that deferasirox (particularly at 20 μmol/L) is more than twofold more efficient in inducing apoptosis in the $CD34^+CD38^-$ cells than in the $CD34^+CD38^+$ cells (Figures 3E and 3F). These results suggest that $CD34^+CD38^-$ KG-1a cells are significantly more sensitive to deferasirox in terms of apoptosis compared with $CD34^+CD38^+$ cells. In addition, deferasirox treatment led to an increase in cleaved caspase-3 and even more prominently in cleaved PARP (a downstream target of caspase-3) (Figure 3G), indicating that this deferasirox-induced apoptosis is most likely caspase dependent.

As shown with the cell line, a 72 hour exposure to deferasirox induced apoptosis in a dose-dependent manner in AML patients' $CD34^+CD38^-CD123^+$ cells (5 μmol/L deferasirox δ between treated and control = 32.5 ± 3.6%, $p < 0.01$; 20 μmol/L deferasirox $\delta = 41$ ± 4.5%, $p < 0.001$) (Figure 3H). Furthermore, the increment in apoptosis of $CD34^+CD38^-CD123^+$ cells exposed to deferasirox (particularly with 20 μmol/L deferasirox) was more than twofold higher ($p < 0.05$) compared with that of the $CD34^+CD38^+CD123^+$ progenitor cells (Figure 3H). These data indicate that deferasirox is highly cytotoxic to AML cells; however, it is significantly more specific to the AML $CD34^+CD38^-CD123^+$ cells. Interestingly, our data also show that the $CD34^+CD38^+CD123^+$ cells exhibited higher sensitivity to ARA-C treatment compared with the more primitive $CD34^+CD38^-CD123^+$ cells (Figure 3H). These data are consistent with studies showing that $CD34^+CD38^-CD123^+$ cells may be resistant to chemotherapy [6–15]. However, the combination of deferasirox and ARA-C induced high levels of apoptosis in both the $CD34^+CD38^-CD123^+$ and the $CD34^+CD38^+CD123^+$ populations, suggesting a synergistic effect between deferasirox and ARA-C (Figure 3H).

Deferasirox exposure increases ROS levels in KG-1a $CD34^+CD38^-$ cells and in the AML patient $CD34^+CD38^-CD123^+$ cell population

Primitive AML cells are more sensitive to changes in oxidative state than the more differentiated counterparts and increased ROS contributes to AML-specific cell death [10]. Deferasirox has been reported to induce ROS generation [32–34], so it could have a major impact on the leukemic $CD34^+CD38^-CD123^+$ cell population through this effect. We therefore examined ROS levels in KG-1a $CD34^+CD38^-$ primitive cells and $CD34^+CD38^+$ cells and in AML patient $CD34^+CD38^-CD123^+$ and $CD34^+CD38^+CD123^+$ progenitor cells following exposure to 5 μmol/L and 20 μmol/L deferasirox for 3 hours using H_2DCFDA. Relative ROS levels were calculated as the fold change of median fluorescence intensity over unstained control. As seen in Figures 4A and 4B, a progressive

Figure 3. Deferasirox induces apoptosis. Apoptosis of KG-1a $CD34^+CD38^-$ and $CD34^+CD38^+$ fractions was evaluated by flow cytometry using Annexin V and 7-AAD. Percentages of apoptotic cells (Annexin V+) and representative dot plots for 24 hours **(A,B)**, 48 hours **(C,D)**, and 72 hours **(E,F)** of exposure to deferasirox are presented. Values represent a mean of three experiments ± SEM. $*p < 0.05$, $**p < 0.01$. **(G)** Quantitative analysis of PARP, cleaved PARP, and cleaved caspase-3 protein levels from $CD34^+CD38^-$ KG-1a cells exposed to deferasirox for 48 hours, accompanied by a representative Western blot. **(H)** $CD34^+CD38^-CD123^+$ and $CD34^+CD38^+CD123^+$ cells isolated from newly diagnosed AML patients (patient samples: AML8, AML9, AML10, and AML27) were cultured with 5 μmol/L and 20 μmol/L deferasirox and/or 0.05 μmol/L ARA-C. Apoptosis was evaluated following 72 hours by flow cytometry using Annexin V. Percentages of apoptotic cells (Annexin V+) are presented. Values represent a mean of four AML patient samples ± SEM. One-way ANOVA followed by Bonferroni's post hoc test were used to compere the different treatments within each cell type. Due to the patients' heterogeneity, paired *t* tests were used for the statistical analysis of the differences between the cell types. $*p < 0.05$, $**p < 0.01$, $***p < 0.001$. #Statistical significance compared with control; $^{\#}p < 0.05$, $^{\#\#}p < 0.01$, $^{\#\#\#}p < 0.001$.

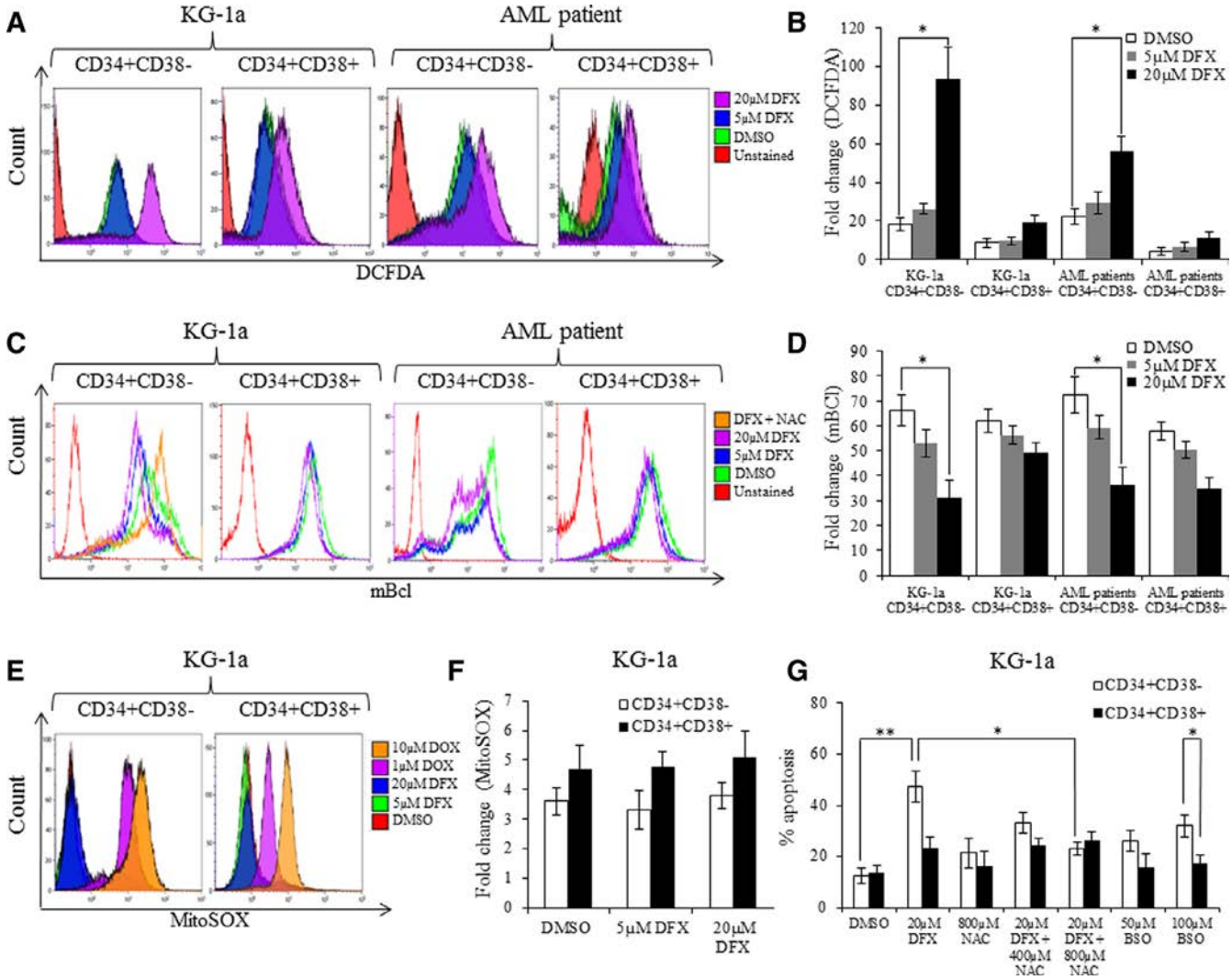

Figure 4. Deferasirox exposure increases ROS levels. KG-1a cells were separated into $CD34^+CD38^-$ and $CD34^+CD38^+$ fractions **(A–G)**. $CD34^+CD38^-CD123^+$ and $CD34^+CD38^+CD123^+$ cells were isolated from newly diagnosed AML patients ($n = 3$) **(A–D)**. All fractions were cultured with 5 μmol/L or 20 μmol/L deferasirox for the indicated times. **(A)** Representative flow cytometric analysis of ROS production using H_2DCFDA staining in KG-1a and AML patient (specimen AML053) cell fractions exposed to deferasirox for 3 hours. **(B)** Relative ROS levels calculated as fold change of median fluorescence intensity over unstained control ± SEM ($n = 3$, patient samples: AML33, AML51, and AML53). **(C)** Representative flow cytometric overlays for mBCl fluorescence from KG-1a and AML patient (specimen AML057) cell fractions exposed to 5 μmol/L or 20 μmol/L deferasirox for 30 min or to 3 hours of 800 μmol/L NAC pretreatment + 30 min of 20 μmol/L deferasirox. **(D)** Relative free thiol groups levels as the fold change of median mBCl fluorescence intensity over unstained control ± SEM ($n = 3$, patient samples: AML54, AML56, and AML57). **(E)** Representative flow cytometric overlays for MitoSOX fluorescence of $CD34^+CD38^-$ and $CD34^+CD38^+$ KG-1a cells exposed to 5 μmol/L or 20 μmol/L deferasirox for 30 min. Exposure to 1–10 μmol/L doxorubicin for 18 hours was used as a positive control. **(F)** Relative superoxide levels as the fold change of median MitoSox fluorescence intensity over unstained control ± SEM ($n = 3$). **(G)** $CD34^+CD38^-$ and $CD34^+CD38^+$ KG-1a cells were exposed to 20 μmol/L deferasirox for 48 hours or pretreated with 400 μmol/L or 800 μmol/L NAC for 1 hour, then washed and treated with 20 μmol/L deferasirox for 48 hours or exposed to 50-100 μmol/L BSO for 48 hours. Apoptosis was evaluated by flow cytometry using Annexin V and 7-AAD. Percentages of apoptotic cells (Annexin V+) are presented ± SEM ($n = 3$). One-way ANOVA followed by Bonferroni's post hoc test were used to compare the different treatments. $^*p < 0.05$, $^{**}p < 0.01$.

increase in ROS levels was seen in the cell line as well as in the AML patients' more primitive cells, in contrast to a more modest increase in ROS levels observed in the more differentiated KG-1a and AML patients cells. ROS levels increased significantly in the $CD34^+CD38^-$ KG-1a cells from the basal level of 18.1 ± 3.4 to 26.3 ± 2.8 and 93.3 ± 16.5 and in the AML patients $CD34^+CD38^-CD123^+$ cells from 22.3 ± 4.3 to 29.4 ± 5.6 and 56.3 ± 7.2 following treatment with 5 μmol/L and 20 μmol/L deferasirox, respectively. In contrast to deferasirox, ARA-C did

not significantly affect ROS levels in the different KG-1a cell populations (data not shown).

Next, we labeled the cells with mBCl, which detects free thiol groups. Reduced labeling intensity signifies loss of free thiols, indicating increased oxidative stress. A reduction in mBCl labeling was evident in the KG-1a $CD34^+CD38^-$ cells and in the AML patients' $CD34^+CD38^-CD123^+$ cells as early as 30 minutes after exposure to deferasirox (Figures 4C and 4D). The reduction in mBCl labeling in the KG-1a $CD34^+CD38^-$ cells supports our KG1a H_2DCFDA staining results. Additionally, we stained the cells with the mitochondrial superoxide indicator MitoSOX red which is oxidized by mitochondrial superoxide but not by non-mitochondrial ROS. Doxorubicin, an inducer of mitochondrial ROS, was used as positive control [38]. As seen in Figures 4E and 4F, no significant change was detected in the superoxide level of the different cells following exposure to deferasirox for 3 hours. These results imply that there is no mitochondrial involvement in the early deferasirox-induced elevation in ROS levels in these cells.

To determine whether the cytotoxic effect of deferasirox is dependent on its ability to increase ROS generation, we pretreated the cells with 400 μmol/L or 800 μmol/L N-acetyl-cysteine (NAC), a potent antioxidant. The cells were then washed and cultured with 20 μmol/L deferasirox for an additional 48 hours. NAC effectively reduced deferasirox-induced apoptosis (Figure 4G). Moreover, NAC reversed the reduction in mBCl labeling that was seen with deferasirox treatment alone and even intensified it over the control (Figure 4C). To study whether the mere increase in ROS levels is responsible for the apoptotic effect seen after deferasirox treatment, KG-1a cells were exposed to 50 μmol/L and 100 μmol/L L-buthionine sulphoximine (BSO) (induces ROS overproduction). The $CD34^+CD38^-$ KG-1a cells were found to be significantly more sensitive to BSO treatment compared with the $CD34^+CD38^+$ cells in terms of apoptosis ($CD34^+CD38^-$: 50 μmol/L BSO 26.3 ± 4.9%, 100 μmol/L BSO 32 ± 6.3%, $CD34^+CD38^+$: 50 μmol/L BSO 15.8 ± 2.3%, 100 μmol/L BSO 17.3 ± 4.2%) (Figure 4G). These data suggest that elevated ROS production by deferasirox could be at least partially responsible for the cytotoxicity that this agent displays against $CD34^+CD38^-$ KG-1a cells.

Deferasirox inhibits NF-κB translocation to the nucleus and downregulates HIF1α expression

NF-κB is activated in primitive AML cells, but not in normal hematopoietic stem cells [9,22,23]. Furthermore, the inhibition of NF-κB signaling induces apoptosis in AML blasts [10,25,26]. Considering that deferasirox is a powerful NF-κB inhibitor [31], it is possible that deferasirox exerts its effect through NF-κB inhibition. We studied the effect of deferasirox on the nuclear localization of NF-κB. $CD34^+CD38^-$ KG-1a cells were exposed to 5 μmol/L and 20 μmol/L deferasirox, 100 μmol/L BSO each for 48 hours, or pretreated with NAC for 1 hour and then washed and exposed to 20 μmol/L deferasirox for 48 hours. Our data revealed a substantial decrease of > 80% ($p < 0.01$) in p65 nuclear levels following 20 μmol/L deferasirox exposure (Figures 5A and 5B). Pretreating the cells with NAC did not reverse the reduction in p65 nuclear levels seen following deferasirox treatment. In addition, treating the cells with BSO slightly increased p65 nuclear and cytoplasmic levels. These data signify that deferasirox exposure leads to a decrease in p65 nuclear expression that is not mediated through deferasirox-induced ROS production. NF-κB regulates the expression of HIF1α [27] and the downregulation of HIF1α has been shown to lead to the elimination of $CD34^+CD38^-$ cells [29]. As seen in Figure 5C, exposure of $CD34^+CD38^-$ KG-1a cells to 20 μmol/L deferasirox for 48 hours significantly reduced the binding of NF-κB to the HIF1α promoter as detected by ChIP assay. In addition, HIF1α mRNA expression was reduced by 40% ($p < 0.01$) (Figure 5D). A similar trend was observed in $CD34^+CD38^-CD123^+$ cells acquired from AML patients with a 55% reduction in HIF1α mRNA expression ($p < 0.01$) (Figure 5E). Additionally, because the hypoxic niches in bone marrow are enriched with leukemic $CD34^+CD38^-$ cells [6] and the HIF1α protein is stabilized under hypoxic conditions, we investigated the effect of hypoxia on KG-1a $CD34^+CD38^-$ and $CD34^+CD38^+$ cells. We observed a significant 70% and 74% decrease in HIF1α protein levels in the KG-1a $CD34^+CD38^-$ cell fraction following a 48 hour exposure to 20 μmol/L deferasirox under normoxic and hypoxic conditions, respectively (Figures 5F and 5G). Interestingly, we did not observe any significant decrease in HIF1α mRNA or protein levels in the more mature $CD34^+CD38^+$ KG-1a cells (Figures 5D, 5F, and 5G) or in the $CD34^+CD38^+CD123^+$ AML patient progenitor cells (Figure 5E). Moreover, under these conditions, we observed a 57% reduction of GLUT1 mRNA expression (transcriptionally regulated by HIF1α [39]) in the KG-1a $CD34^+CD38^-$ cells ($p < 0.01$) (Figure 5H). Basal HIF1α mRNA and protein levels were significantly higher in the $CD34^+CD38^-$ cell fraction (of both the cell line and patient samples) compared with the $CD34^+CD38^+$ cells (Figures 5D–5G). These data, combined with previous reports that the more mature leukemic cells are less sensitive to HIF1α downregulation [28,29], may suggest that HIF1α expression is more crucial for the maintenance of $CD34^+CD38^-CD123^+$ cells compared with the more mature cells and that deferasirox exerts its effect on the $CD34^+CD38^-CD123^+$ cells at least in part through this pathway.

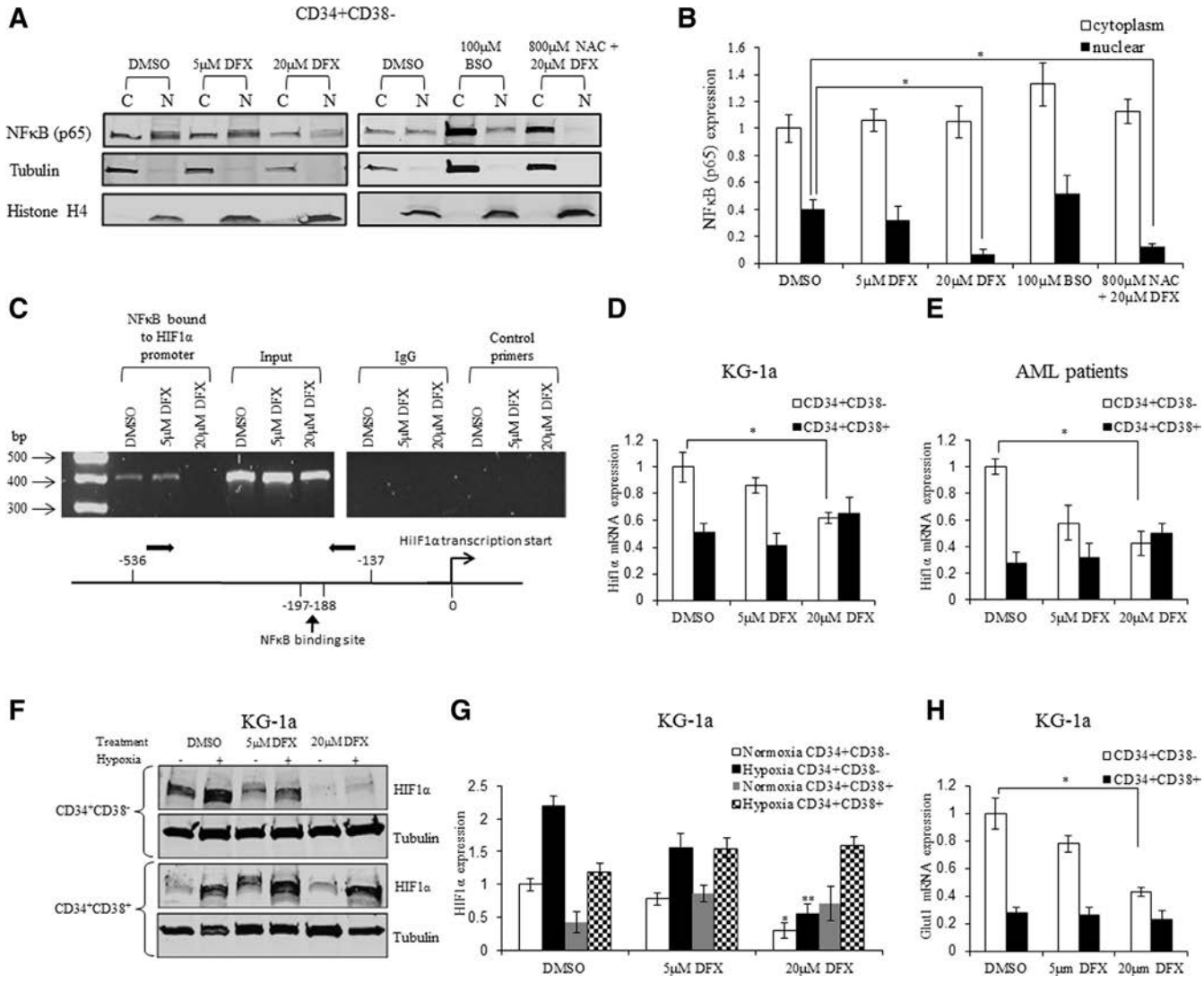

Figure 5. Deferasirox downregulates HIF1α expression. $CD34^+CD38^-$ and $CD34^+CD38^+$ KG-1a fractions were exposed to 5 μmol/L and 20 μmol/L deferasirox or exposed to 100 μmol/L BSO for 48 hours or pretreated with 800 μmol/L NAC for 1 hour, then washed and treated with 20 μmol/L deferasirox for 48 hours. Nuclear and cytoplasmic fractions were analyzed using anti-p65. Anti-β-tubulin and anti-histone-H4 were used to assess fractionation efficiency. **(A)** Representative Western blots. **(B)** Quantification of p65 expression. Values represent the mean of three experiments ± SEM. One-way ANOVA followed by Bonferroni's post hoc test were used to compare the different treatments. *$p <$ 0.01. **(C)** $CD34^+CD38^-$ KG-1a cells were treated with deferasirox for 48 hours and recruitment of NF-κB to the HIF1α proximal promoter was evaluated by ChIP. Anti-p65 antibody was used for immunoprecipitation. PCR was performed with primers spanning the HIF1α proximal promoter. Shown is a representative PCR experiment. **(D)** Real-time PCR of HIF1α in $CD34^+CD38^-$ and $CD34^+CD38^+$ KG-1a cells. **(E)** Real-time PCR of HIF1α in $CD34^+CD38^-CD123^+$ and $CD34^+CD38^+CD123^+$ cells isolated from newly diagnosed AML patients ($n = 3$, patient samples: AML27, AML51, and AML58). **(F)** KG-1a $CD34^+CD38^-$ and $CD34^+CD38^+$ cell fractions were treated with deferasirox and subjected to hypoxic/normoxic conditions for 48 hours. Representative Western blot of HIF1α in KG-1a cells is shown. **(G)** Quantitative analysis of HIF1α protein levels. Values represent a mean of three experiments ± SEM. *$p < 0.05$**$p < 0.01$. **(H)** Real-time PCR of GLUT1 in KG-1a cells. Values represent a mean of three experiments ± SEM.*$p < 0.01$.

HIF1α downregulation in combination with ROS induction and iron chelation is required for apoptosis induction in KG-1a $CD34^+CD38^-$ cells

At this point, we were interested in determining whether the combined ability of deferasirox to chelate iron, increase ROS production (Figure 4), and reduce HIF1α expression (Figure 5) is responsible for the selective apoptosis seen in the KG-1a $CD34^+CD38^-$ cells. We therefore tested the ability of these three properties separately and combined to induce apoptosis in $CD34^+CD38^-$ KG-1a cells and in the $CD34^+CD38^+$ KG-1a cells. We used BSO to induce ROS overproduction, si-HIF1α to reduce HIF1α levels, and the chelator deferiprone (known to chelate iron but not to reduce NF-κB expression [31]) to reduce iron levels. si-HIF1α-transfected KG-1a $CD34^+CD38^-$ cells showed an ~60% reduction in HIF1α mRNA expression (Figure 6A),

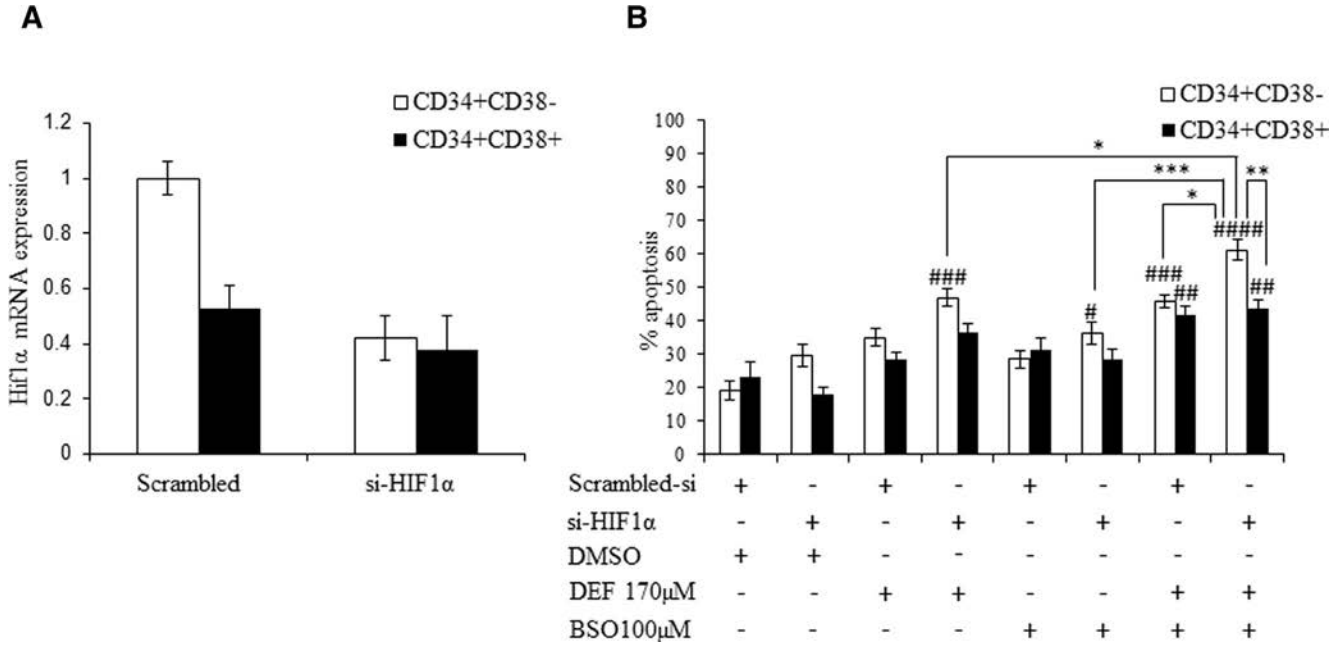

Figure 6. HIF1α downregulation in combination with ROS production and iron chelation induces apoptosis in KG-1a $CD34^+CD38^-$ cells. $CD34^+CD38^-$ and $CD34^+CD38^+$ fractions were treated with si-HIF1α, scrambled siRNA, BSO, deferiprone (DEF), or DMSO. **(A)** Real-time PCR of HIF1α 24 hours after si-HIF1α transfection. **(B)** Twenty-four hours after si-transfections, the cells were treated with 170 μmol/L DEF and/or with 100 μmol/L BSO for 48 hours. Apoptosis was evaluated by Annexin V. Percentages of apoptotic cells (Annexin V+) are presented. One-way ANOVA followed by Bonferroni's post hoc test were used to compere the different treatments. *$p < 0.05$, **$p < 0.01$, ***$p < 0.001$. #Statistical significance compared with control; $^{\#}p < 0.05$, $^{\#\#}p < 0.01$, $^{\#\#\#}p < 0.001$, $^{\#\#\#\#}p < 0.0001$.

which is similar to the effect that deferasirox had on HIF1α mRNA expression in these cells (Figure 5A). Transfection of si-HIF1α slightly increased the apoptotic population of the $CD34^+CD38^-$ KG-1a cells and did not alter the apoptotic population of the $CD34^+CD38^+$ cells. Exposing the cells to 170 μmol/L deferiprone also did not have a statistically significant apoptotic effect on the $CD34^+CD38^-$ KG-1a cells or on the $CD34^+CD38^+$ cells. Similarly, exposing the cells to BSO did not culminate in significant apoptosis (Figure 6B). si-HIF1α-transfected cells exposed to deferiprone or to BSO displayed a significant apoptotic response only in the $CD34^+CD38^-$ fraction. However, exposure to BSO and deferiprone together resulted in a significant apoptotic response in both the $CD34^+CD38^-$ and $CD34^+CD38^+$ KG-1a cells. Interestingly, treating si-HIF1α-transfected cells with BSO and deferiprone led to an apoptotic response in the $CD34^+CD38^-$ cells that was significantly greater than that seen in the $CD34^+CD38^+$ cells. Moreover, the apoptotic response of the si-HIF1α-transfected $CD34^+CD38^+$ cells treated with BSO and deferiprone was similar to that of the scrambled transfected $CD34^+CD38^+$ cells treated with BSO and deferiprone (Figure 6B). These data imply that the particular combined ability of deferasirox to chelate iron, induce ROS production, and reduce HIF1α expression facilitates its ability to induce apoptosis specifically in the $CD34^+CD38^-$ cell fraction.

Discussion

The AML $CD34^+CD38^-$ cell population is highly resistant to conventional chemotherapies and this resistance may contribute to AML treatment failure. Guzman et al. [40] proposed that two types of events are necessary to induce preferential $CD34^+CD38^-CD123^+$ cell death: (1) inhibition of survival signals (such as NF-κB) and (2) activation of stress responses (such as oxidative stress response). We showed that clinically relevant concentrations of deferasirox, a Food and Drug Administration-approved iron chelator, specifically targets the leukemic $CD34^+CD38^-CD123^+$ cell fraction by inhibiting NF-κB and HIF1α and by increasing ROS levels. We also showed that these events are not directly linked to each other because NF-κB nuclear localization, and thus activation, was not reduced following exposure of the cells to BSO. In addition, the generation of ROS was observed within minutes following exposure to deferasirox and thus is probably not mediated by a slow, NF-κB-dependent transcriptional activation response.

It is important to mention that, throughout our experiments, the KG-1a cells behaved in a similar manner to the AML samples. The AML patient $CD34^+CD38^-CD123^+$ cells and the $CD34^+CD38^-$ KG-1a cells were more sensitive to deferasirox in terms of apoptosis, NF-κB, and

HIF1α downregulation and increment of ROS compared with the progenitor leukemic cells.

A surprising result was that, even though deferasirox displayed an apoptotic effect primarily on primitive KG-1a and AML cells, its anti-proliferative effect was detected on both the primitive and more mature cells. BrdU pulse assay showed that DNA transcription decreased rather quickly. This immediate response may indicate the existence of an additional, yet to be established mechanisms by which deferasirox exerts this specific effect. Importantly, studies have shown that deferasirox, at concentrations equal to those we used or even at higher ones, has no effect on normal hematopoietic stem cell's viability [32,33]. Moreover, clinical studies that tested the effect of deferasirox treatment on aplastic anemia, myelodysplastic syndromes (MDS), and post-bone marrow transplantation patients showed a favorable hematological response to deferasirox treatment, with positive blood counts, which suggests that hematopoietic stem cells are unaffected by this treatment [41–43].

We believe that deferasirox exerts its cytotoxic effect at least in part by downregulating HIF1α levels in the $CD34^+CD38^-CD123^+$ population via inhibiting the translocation of NF-κB to the nucleus. Generally, high HIF1α expression is correlated with tumor growth, therapy resistance, and relapse [44,45]. Therefore, sustained expression of HIF1α can be considered a marker for poor prognosis in AML and other hematological malignancies [46–50]. Furthermore, several studies have shown that the inhibition of HIF1α results in the failure of malignant primary cells to form in vitro colonies and even significantly increases disease-free survival in vivo [28,29,48,51,52]. However, the specific role of HIFs in hematological malignancies seems to be controversial and contradictory data have been published. Several studies have reported that HIF1α expression may induce cell differentiation in AML and low levels of HIF1α may correlate with reduced survival [53–55]. This discrepancy may be explained by the use of different models (mouse vs. human) and short hairpin RNA-inhibiting drugs compared with knock-out models. Interestingly, the mere downregulation of HIF1α did not induce a significant apoptotic response in the KG-1a $CD34^+CD38^-$ cells, which is contradictory to previous studies showing that targeting HIF1α eliminates cancer stem cells in hematological malignancies [28,29]. This discrepancy may emanate from the fact that, in the previous studies [28,29], HIF1α expression was severely reduced to levels substantially lower than those in our experiments. In our studies, we ensured an accurate HIF1α expression level obtained following exposure to clinically relevant concentration of deferasirox, which was 50–60% of the normal expression level. We found that this amount of downregulation is sufficient to induce apoptosis in the $CD34^+CD38^-$ cells only when combined with the iron chelator deferiprone, which does not have an effect on NF-κB, and with BSO. We therefore believe that deferasirox utilizes a combination of HIF1α downregulation, ROS induction, and iron chelation to induce apoptosis in these cells.

An additional interesting finding was that deferasirox induced ROS generation in the KG-1a and AML patients' $CD34^+CD38^-$ cells and exposure to NAC substantially diminished deferasirox-mediated cell death. In addition, the $CD34^+CD38^-$ KG-1a cells were much more sensitive to BSO treatment compared with the more mature cells. These data indicate that increased ROS contributes to $CD34^+CD38^-$ specific cell death triggered by deferasirox and that the observed cell death may even be dependent on this specific characteristic of deferasirox. mBcl staining revealed a rapid decrease in free thiol groups following exposure to deferasirox, which indicates a very prompt induction in ROS levels. This immediate effect is most likely not a result of the activation of complicated and time-consuming molecular pathways, but rather is a direct effect. An immediate and direct effect of iron chelators have been described previously, such as seen with di-2-pyridylketone isonicotinoyl hydrazone, which generates ROS in a mitochondria-independent process by enhancing Fenton chemistry, thus promoting the production of Fenton-derived radicals [56].

Iron participates in the Fenton reaction, which generates hydroxyl radicals. Deferasirox would therefore be expected to lower intracellular ROS levels. Consistent with this hypothesis, a clinical trial showed reduced ROS levels in red blood cells of MDS patients after 3 months of deferasirox therapy [57,58]. However, several studies of variable in vitro effects of deferasirox on cellular ROS levels in MDS/AML have been published [32–34,59]. In these studies, whenever the cells were exposed to deferasirox for very short periods (30 minutes), an increase in ROS levels was detected [32,34]. In cases in which the cells were exposed to deferasirox for longer periods (24–72 hours), ROS levels were decreased [59]. Based on these studies, iron chelators seem to initiate pro-oxidant and anti-oxidant effects. One possible explanation for this phenomenon is that iron chelators will always induce an initial increase in ROS levels. In some cells, this will trigger antioxidant response pathways that will ultimately lead to a decrease in ROS levels. In other cells, such as our $CD34^+CD38^-$ cells, these pathways may be inhibited and the increase in ROS will eventually activate an apoptotic response.

Interestingly, many chemotherapeutic agents are known to increase ROS, but such agents also typically upregulate NF-κB activity. NF-κB is a key component in the cells' adjustment to high oxidative stress [60]. Because

deferasirox elevates ROS levels and inhibits NF-κB activity, deferasirox may sensitize the $CD34^+CD38^-$ cells to the increase in ROS. If this assumption is accurate, then it might explain the chemosensitizing effect that we observed when combining deferasirox with ARA-C. Moreover, this sort of interaction might occur with other common anti-leukemia drugs [26,61] and this unique inhibition in NF-κB activity could explain the inability of these $CD34^+CD38^-$ cells to properly activate antioxidant pathways in response to high ROS levels.

Over the past decade, several studies have demonstrated the promising yet limited cytotoxic potential of deferasirox against leukemic cell lines [31,34,59]. In the clinical setting, retrospective studies in MDS patients suggested that iron chelators may increase life expectancy and decrease the risk of transformation into AML [62,63]. In another study, AML patients failing hypomethylating agents were treated with deferasirox and vitamin D. Their overall survival significantly increased compared with matched patients receiving best supportive care only [64]. Additionally, a 2011 case study described a patient with chemotherapy-resistant AML, who achieved complete remission after being treated only with deferasirox [65]. The molecular mechanism in all of these cases remains unknown.

We describe a novel anti-$CD34^+CD38^-$ property of deferasirox. We found clinically relevant concentrations of deferasirox to be cytotoxic in vitro to AML progenitor cells, but even more potent against the $CD34^+CD38^-CD123^+$ cell population. We believe that deferasirox exerts its cytotoxic effect at least in part by downregulating HIF1α levels in the leukemic $CD34^+CD38^-CD123^+$ population and by increasing ROS levels. Pending further characterization, deferasirox can be considered as a potential therapeutic agent for eradicating $CD34^+CD38^-CD123^+$ cells.

Acknowledgments

This work was supported by the Israeli Cancer Association, the Sapon Foundation, and REUT (the Association for Advancement in Medicine in Israel).

Conflict of interest disclosure

The authors declare no competing financial interests.

References

1. Bonnet D, Dick JE. Human acute myeloid leukemia is organized as a hierarchy that originates from a primitive hematopoietic cell. Nat Med. 1997;3:730–737.
2. Buchner T, Berdel WE, Haferlach C, et al. Age-related risk profile and chemotherapy dose response in acute myeloid leukemia: a study by the German Acute Myeloid Leukemia Cooperative Group. J Clin Oncol. 2009;27:61–69.
3. Fernandez HF, Sun Z, Yao X, et al. Anthracycline dose intensification in acute myeloid leukemia. N Engl J Med. 2009;361:1249–1259.
4. Burnett AK, Hills RK, Milligan DW, et al. Attempts to optimize induction and consolidation treatment in acute myeloid leukemia: results of the MRC AML12 trial. J Clin Oncol. 2010;28:586–595.
5. Dombret H, Gardin C. An update of current treatments for adult acute myeloid leukemia. Blood. 2016;127:53–61.
6. Saito Y, Uchida N, Tanaka S, et al. Induction of cell cycle entry eliminates human leukemia stem cells in a mouse model of AML. Nat Biotechnol. 2010;28:275–280.
7. Ho MM, Hogge DE, Ling V. MDR1 and BCRP1 expression in leukemic progenitors correlates with chemotherapy response in acute myeloid leukemia. Exp Hematol. 2008;36:433–442.
8. Costello RT, Mallet F, Gaugler B, et al. Human acute myeloid leukemia $CD34^+/CD38^-$ progenitor cells have decreased sensitivity to chemotherapy and Fas-induced apoptosis, reduced immunogenicity, and impaired dendritic cell transformation capacities. Cancer Res. 2000;60:4403–4411.
9. Guzman ML, Neering SJ, Upchurch D, et al. Nuclear factor-kappaB is constitutively activated in primitive human acute myelogenous leukemia cells. Blood. 2001;98:2301–2307.
10. Guzman ML, Rossi RM, Karnischky L, et al. The sesquiterpene lactone parthenolide induces apoptosis of human acute myelogenous leukemia stem and progenitor cells. Blood. 2005;105:4163–4169.
11. Ishikawa F, Yoshida S, Saito Y, et al. Chemotherapy-resistant human AML stem cells home to and engraft within the bone-marrow endosteal region. Nat Biotechnol. 2007;25:1315–1321.
12. van Rhenen A, Feller N, Kelder A, et al. High stem cell frequency in acute myeloid leukemia at diagnosis predicts high minimal residual disease and poor survival. Clin Cancer Res. 2005;11:6520–6527.
13. Witte KE, Ahlers J, Schäfer I, et al. High proportion of leukemic stem cells at diagnosis is correlated with unfavorable prognosis in childhood acute myeloid leukemia. Pediatr Hematol Oncol. 2011;28:91–99.
14. Vergez F, Green AS, Tamburini J, et al. High levels of $CD34^+CD38low/-CD123^+$ blasts are predictive of an adverse outcome in acute myeloid leukemia: a Groupe Ouest-Est des Leucemies Aigues et Maladies du Sang (GOELAMS) study. Haematologica. 2011;12:1792–1798.
15. Wang L, Gao L, Xu S, et al. FISH+CD34+CD38- cells detected in newly diagnosed acute myeloid leukemia patients can predict the clinical outcome. J Hematol Oncol. 2013;7;6(1):85.
16. Gerber JM, Smith BD, Ngwang B, et al. A clinically relevant population of leukemic $CD34^+CD38^-$ cells in acute myeloid leukemia. Blood. 2012;119:3571–3577.
17. Sarry JE, Murphy K, Perry R, et al. Human acute myelogenous leukemia stem cells are rare and heterogeneous when assayed in NOD/SCID/IL2Rgammac-deficient mice. J Clin Invest. 2011;121:384–395.
18. van Rhenen A, Moshaver B, Kelder A, et al. Aberrant marker expression patterns on the $CD34^+CD38^-$ stem cell compartment in acute myeloid leukemia allows to distinguish the malignant from the normal stem cell compartment both at diagnosis and in remission. Leukemia. 2007;21:1700–1707.
19. Feller N, van der Pol MA, van Stijn A, et al. MRD parameters using immunophenotypic detection methods are highly reliable in predicting survival in acute myeloid leukaemia. Leukemia. 2004;18:1380–1390.
20. Zhang B, Strauss AC, Chu S, et al. Effective targeting of quiescent chronic myelogenous leukemia stem cells by histone deacetylase inhibitors in combination with imatinib mesylate. Cancer Cell. 2010;17:427–442.
21. Takahashi-Yanaga F, Kahn M. Targeting Wnt signaling: can we safely eradicate cancer stem cells? Clin Cancer Res. 2010;16:3153–3162.

22. Estrov Z, Manna SK, Harris D, et al. Phenylarsine oxide blocks interleukin-1beta-induced activation of the nuclear transcription factor NF-kappaB, inhibits proliferation, and induces apoptosis of acute myelogenous leukemia cells. Blood. 1999;94:2844–2853.
23. Baumgartner B, Weber M, Quirling M, et al. Increased IkappaB kinase activity is associated with activated NF-kappaB in acute myeloid blasts. Leukemia. 2002;16:2062–2071.
24. Bassères DS, Baldwin AS. Nuclear factor-kappaB and inhibitor of kappaB kinase pathways in oncogenic initiation and progression. Oncogene. 2006;25:6817–6830.
25. Guzman ML, Swiderski CF, Howard DS, et al. Preferential induction of apoptosis for primary human leukemic stem cells. Proc Natl Acad Sci U S A. 2002;99:16220–16225.
26. Frelin C, Imbert V, Griessinger E, et al. Targeting NF-kappaB activation via pharmacologic inhibition of IKK2-induced apoptosis of human acute myeloid leukemia cells. Blood. 2005;105:804–811.
27. Van Uden P, Kenneth N, Rocha S. Regulation of hypoxia-inducible factor-1alpha by NF-kappaB. Biochem J. 2008;412:477–484.
28. Haojian Z, Huawei L, Hualin X, Shaoguang L. HIF1α is required for survival maintenance of chronic myeloid leukemia stem cells. Blood. 2012;10:381–387.
29. Wang Y, Liu Y, Malek S, Zheng P, Liu Y. Targeting HIF1α eliminates cancer stem cells in hematological malignancies. Cell Stem Cell. 2011;8:399–411.
30. Yang LP, Keam SJ, Keating GM. Deferasirox: a review of its use in the management of transfusional chronic iron overload. Drugs. 2007;67:2211–2230.
31. Messa E, Carturan S, Maffè C, et al. Deferasirox is a powerful NF-kappaB inhibitor in myelodysplastic cells and in leukemia cell lines acting independently from cell iron deprivation by chelation and reactive oxygen species scavenging. Haematologica. 2010;95:1308–1316.
32. Tataranni T, Aqriesti F, Mazzoccoli C, et al. The iron chelator deferasirox affects redox signaling in heamatopoietic stem/progenitor cells. Br J Haematol. 2015;170:236–246.
33. Pullarkat V, Sehgal A, Li L, et al. Deferasirox exposure induces reactive oxygen species and reduces growth and viability of myelodysplastic hematopoietic progenitors. Leuk Res. 2012;36:966–973.
34. Callens C, Coulon S, Naudin J, et al. Targeting iron homeostasis induces cellular differentiation and synergizes with differentiating agents in acute myeloid leukemia. J Exp Med. 2010;207:731–750.
35. She M, Niu X, Chen X, et al. Resistance of leukemic stem-like cells in AML cell line KG1a to natural killer cell-mediated cytotoxicity. Cancer Lett. 2012;318:173–179.
36. Vazana-Barad L, Granot G, Mor-Tzuntz R, et al. Mechanism of the antitumoral activity of deferasirox, an iron chelation agent, on mantle cell lymphoma. Leuk Lymphoma. 2013;54:851–859.
37. Piga A, Galanello R, Forni GL, et al. Randomized phase II trial of deferasirox (Exjade, ICL670), a once-daily, orally-administered iron chelator, in comparison to deferoxamine in thalassemia patients with transfusional iron overload. Haematologica. 2006;91:873–880.
38. Mukhopadhyay P, Rajesh M, Hasko G, Hawkins BJ, Madesh M, Pacher P. Simultaneous detection of apoptosis and mitochondrial superoxide production in live cells by flow cytometry and confocal microscopy. Nat Protoc. 2007;2:2295–2301.
39. Chen C, Pore N, Behrooz A, Ismail-Beigi F, Maity A. Regulation of glut1 mRNA by hypoxia-inducible factor-1. Interaction between H-ras and hypoxia. J Biol Chem. 2001;276:9519–9525.
40. Guzman ML, Rossi RM, Neelakantan S, et al. An orally bioavailable parthenolide analog selectively eradicates acute myelogenous leukemia stem and progenitor cells. Blood. 2007;110:4427–4435.
41. Gattermann N, Finelli C, Della Porta M. Hematologic responses to deferasirox therapy in transfusion-dependent patients with myelodysplastic syndromes. Haematologica. 2012;97:1364–1371.
42. Lee JW, Yoon SS, Shen ZX. Hematologic responses in patients with aplastic anemia treated with deferasirox: a post hoc analysis from the EPIC study. Haematologica. 2013;98:1045–1048.
43. Visani G, Guiducci B, Giardini C. Deferasirox improves hematopoiesis after allogeneic hematopoietic SCT. Bone Marrow Transplant. 2014;49:585–587.
44. Zhong H, De Marzo AM, Laughner E, et al. Overexpression of hypoxia-inducible factor 1alpha in common human cancers and their metastases. Cancer Res. 1999;59:5830–5835.
45. Trastour C, Benizri E, Ettore F, et al. HIF-1alpha and CA IX staining in invasive breast carcinomas: prognosis and treatment outcome. Int J Cancer. 2007;120:1451–1458.
46. Semenza GL. Targeting HIF-1 for cancer therapy. Nat Rev Cancer. 2003;3:721–732.
47. Deeb G, Vaughan MM, McInnis I, et al. Hypoxia-inducible factor-1α protein expression is associated with poor survival in normal karyotype adult acute myeloid leukemia. Leuk Res. 2011;35:579–584.
48. Gao XN, Yan F, Lin J, et al. AML1/ETO cooperates with HIF1α to promote leukemogenesis through DNMT3a transactivation. Leukemia. 2015;29:1730–1740.
49. Zhe N, Wang J, Chen S, et al. Heme oxygenase-1 plays a crucial role in chemoresistance in acute myeloid leukemia. Hematology. 2015;20:384–391.
50. Song K, Li M, Xu XJ, et al. HIF-1α and GLUT1 gene expression is associated with chemoresistance of acute myeloid leukemia. Asian Pac J Cancer Prev. 2014;15:1823–1829.
51. Coltella N, Percio S, Valsecchi R, et al. HIF factors cooperate with PML-RARα to promote acute promyelocytic leukemia progression and relapse. EMBO Mol Med. 2014;6:640–650.
52. Wang Y, Liu Y, Tang F, et al. Echinomycin protects mice against relapsed acute myeloid leukemia without adverse effect on hematopoietic stem cells. Blood. 2014;124:1127–1135.
53. Liu W, Guo M, Xu YB, et al. Induction of tumor arrest and differentiation with prolonged survival by intermittent hypoxia in a mouse model of acute myeloid leukemia. Blood. 2006;107:698–707.
54. Velasco-Hernandez T, Hyrenius-Wittsten A, Rehn M, Bryder D, Cammenga J. HIF-1α can act as a tumor suppressor gene in murine acute myeloid leukemia. Blood. 2014;124:3597–3607.
55. Velasco-Hernandez T, Tornero D, Cammenga J. Loss of HIF-1α accelerates murine FLT-3(ITD)-induced myeloproliferative neoplasia. Leukemia. 2015;29:2366–2374.
56. Chaston TB, Watts RN, Yuan J, Richardson DR. Potent antitumor activity of novel iron chelators derived from Di-2-pyridylketone isonicotinoyl hydrazone involves Fenton-derived free radical generation. Clin Cancer Res. 2004;10:7365–7374.
57. Ghoti H, Amer Winder A, Rachmilewitz E, Fibach E. Oxidative stress in blood cells, platelets and polymorphonuclear leukocytes from patients with myelodysplastic syndrome. Eur J Haematol. 2007;79:463–467.
58. Ghoti H, Fibach E, Merkel D, Perez-Avraham G, Grisariu S, Rachmilewitz E. Changes in parameters of oxidative stress and free iron biomarkers during treatment with deferasirox in iron overloaded patients with myelodysplastic syndromes. Haematologica. 2010;95:1433–1434.
59. Li N, Chen Q, Gu J, et al. Synergistic inhibitory effects of deferasirox in combination with decitabine on leukemia cell lines SKM-1, THP-1, and K-562. Oncotarget. 2017;8:36517–36530.
60. Morgan MJ, Liu ZG. Crosstalk of reactive oxygen species and NF-κB signaling. Cell Res. 2011;21:103–115.

61. Kanno S, Hiura T, Shouji A, et al. Resistance to Ara-C up-regulates the activation of NF-kappaB, telomerase activity and Fasexpression in NALM-6 cells. Biol Pharm Bul. 2007;30:2069–2074.
62. Malcovati L, Porta MG, Pascutto C, et al. Prognostic factors and life expectancy in myelodysplastic syndromes classified according to WHO criteria: a basis for clinical decision making. J Clin Oncol. 2005;23:7594–7603.
63. Rose C, Brechignac S, Vassilief D, et al. Does iron chelation therapy improve survival in regularly transfused lower risk MDS patients? A multicenter study by the GFM (Groupe Francophone des Myelodysplasies). Leuk Res. 2010;34:864–870.
64. Paubelle E, Zylbersztejn F, Alkhaeir S, et al. Deferasirox and vitamin D improves overall survival in elderly patients with acute myeloid leukemia after demethylating agents failure. PLoS One. 2013;8:e65998.
65. Fukushima T, Kawabata H, Nakamura T, et al. Iron chelation therapy with deferasirox induced complete remission in a patient with chemotherapy-resistant acute monocytic leukemia. Anticancer Res. 2011;31:1741–1744.

Supplementary methods for:

Deferasirox induces cell death in leukemic stem cells through iron chelation, induction of ROS and inhibition of HIF1α expression

Cell isolation and culture. Primary AML cells were obtained, after a written informed consent was granted, from the bone marrow of newly diagnosed AML patients at the Davidoff Center, Rabin Medical Center, Israel and at the Division of Hematology, Sheba Medical Center, Tel Hashomer, Israel. This research was approved by the Rabin Medical Center and the Sheba Medical Center Institutional Review Boards and Ethics Committees and was performed according to the Declaration of Helsinki of 1975 as revised in 1996. The characteristics of the patient samples are summarized in Table 1. Bone marrow samples were separated by Lymphoprep density gradient (Axis-shield, Dundee, Scotland) in order to isolate the mononuclear blood cell compartment. At this point cells were either further separated (see below) or cryopreserved in freezing medium consisting of Iscove's Modified Dulbecco Medium (IMDM) (Sigma Aldrich), 40% fetal bovine serum (FBS), and 10% dimethylsulfoxide (DMSO) (Sigma Aldrich). The human AML cell line KG-1a (kindly provided by Prof. Tsvee Lapidot, Weizmann Institute of Science) was maintained in suspension culture with IMDM supplemented with 20% FBS. For $CD34^+CD38^-$/$CD34^+CD38^+$ cell separation (from the cell line and from patient samples), the CD34 Multi Sort kit (Miltenyi Biotec, Bergisch Gladbach, Germany) applied on a midiMACS immunoaffinity device (Miltenyi Biotec) was used according to the manufacturer's instructions. The purity of the resulting fractions was determined by staining with α-CD34-PE, α-CD38-FITC (Miltenyi Biotec), α-CD123-APC and α-CD38-PE-Cy5 (Thermo-Fisher Scientific, Waltham, MA, USA) and flow cytometric evaluation on a Gallios flow cytometer (Beckman Coulter, Indianapolis, IN, USA). All patient samples were > 85% $CD123^+$ (see Figure 1 for one representative cell isolation experiment). The sorted AML cells were cultured at a starting density of 2×10^5 cells/ml at 37°C, 5% CO_2, in a humidified incubator for 3-4 days in serum-free media consisting of IMDM supplemented with 20% BIT 9500 serum substitute (containing bovine serum albumin (BSA), insulin, and transferrin (BIT)) (Stem Cell Technologies, Vancouver, Canada). The following cytokines were added: 100ng/ml SCF 100ng/ml granulocyte-colony stimulating factor (G-CSF), 20ng/ml FLT-3 ligand, 20ng/ml IL-3, and 20ng/ml IL-6 (PeproTech, Rehovot, Israel). The KG-1a sorted cells were cultured at a starting density of 2×10^5 cells/ml in IMDM supplemented with 20% FBS. Compounds used for cells treatment were: deferasirox, deferipron (Selleckchem, Munich, Germany), N-acetyl-l-cysteine (NAC), ARA-C, Buthionine sulfoximine (BSO) (Sigma Aldrich).

Chromatin immunoprecipitation

Measurement of chromatin immunoprecipitation (ChIP) following incubation of KG-1a cells with deferasirox was performed by Magna-CHIP chromatin immunoprecipitation kit (Millipore, Burlington, MA, USA) according to the manufacturer's instructions. Briefly, cells were grown and treated with formaldehyde in order to crosslink proteins to DNA to ensure co-precipitation. Cross-linking reactions were quenched with glycine, cells were then lysed, and chromatin was sonicated to shear the chromatin to a manageable size of 200−1000bp. The average fragment size was confirmed empirically by gel electrophoresis. Following centrifugation, the chromatin was adequately diluted and pre-cleared with protein G-agarose beads. Pre-cleared chromatin was incubated overnight at 4°C with an antibody

Table 1. Characteristics of the patient samples

Specimen ID	Sex	Age	Cytogenetics	BM blasts (%)	WBC (10^3/L)
AML008	M	58	Trisomy 8	50	4.72
AML009	M	77	CK	80	1.50
AML010	F	26	del7(7q22/7q31), t(11q23)	100	250.0
AML011	M	66	NK	40	37.0
AML015	F	65	t(8;21), −7	70	13.60
AML022	F	39	NK	100	3.70
AML027	F	76	NK	100	8.90
AML033	F	38	Trisomy 8	70	3.07
AML051	M	32	NK	50	97.13
AML053	M	77	Trisomy 8, t(9;11)(p22;q23)	50	22.07
AML054	F	49	CK	24	6.15
AML056	F	37	NA*	50	77.02
AML057	F	35	Trisomy 8	50	12.08
AML058	F	72	t(3;9;22)(p21;q34;q11.2)	25	160.00

F: female; M: male; NK: normal karyotype; CK: complex karyotype; WBC: white blood count; NA: not applicable.
*Due to lack of mitosis karyotype analysis was not performed.

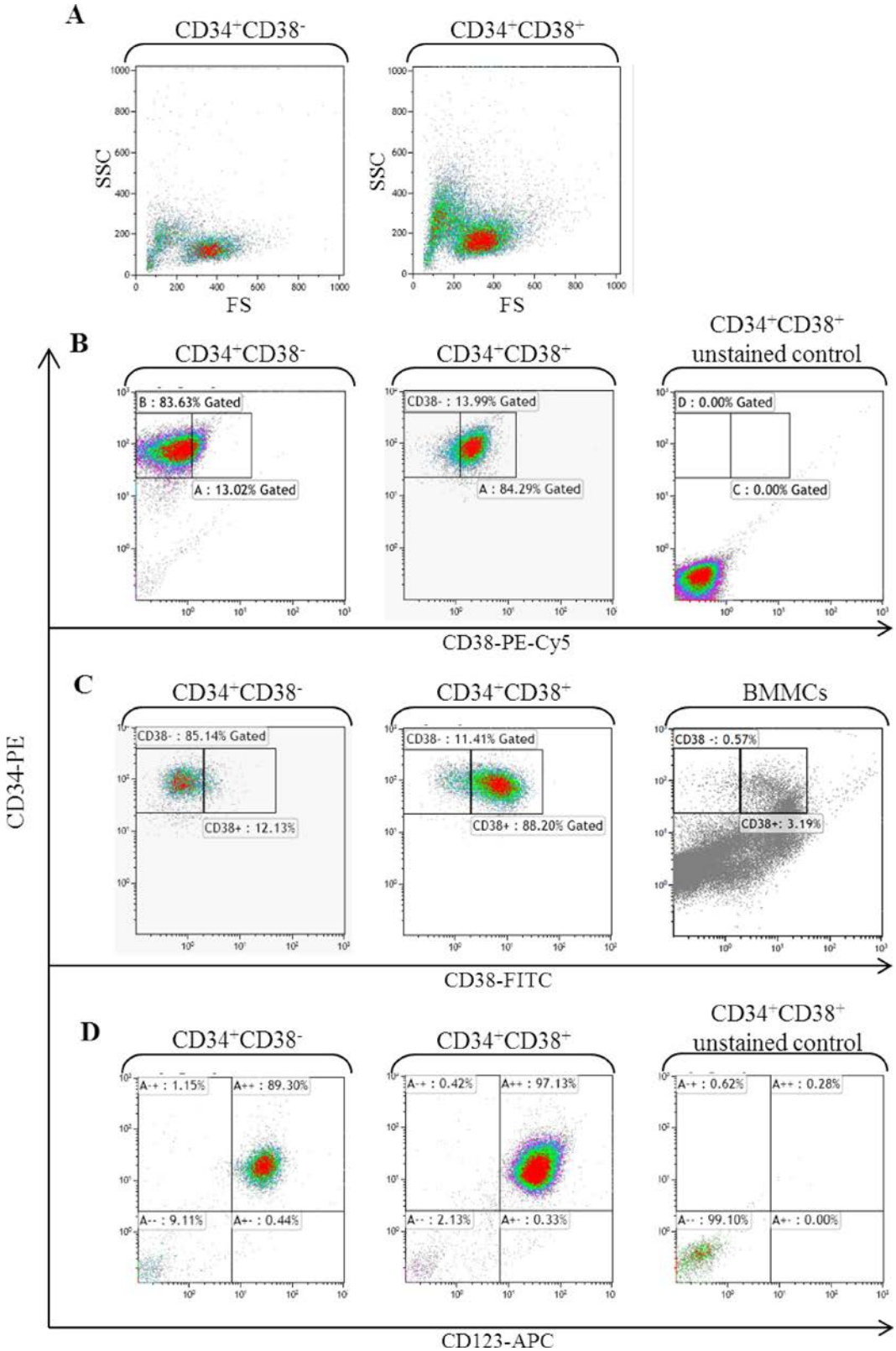

Figure 1. Purification and phenotypic analysis of the CD34$^+$CD38$^-$CD123$^+$/CD34$^+$CD38$^+$CD123$^+$ populations from AML samples. CD34$^+$ cells were isolated from an AML patient's bone marrow sample (AML8). These cells were further sorted into CD34$^+$CD38$^+$ and CD34$^+$CD38$^-$ fractions. Representative dot plots of the two cell fractions are shown: **A.** forward scatter (FS) and side scatter (SSC) characteristics of the isolated cells. **B.** CD34-PE, CD38-PE-Cy5 and unstained control. **C.** CD34-PE, CD38-FITC and bone marrow mononuclear cells (BMMCs). **D.** CD34-PE, CD123-APC and unstained control.

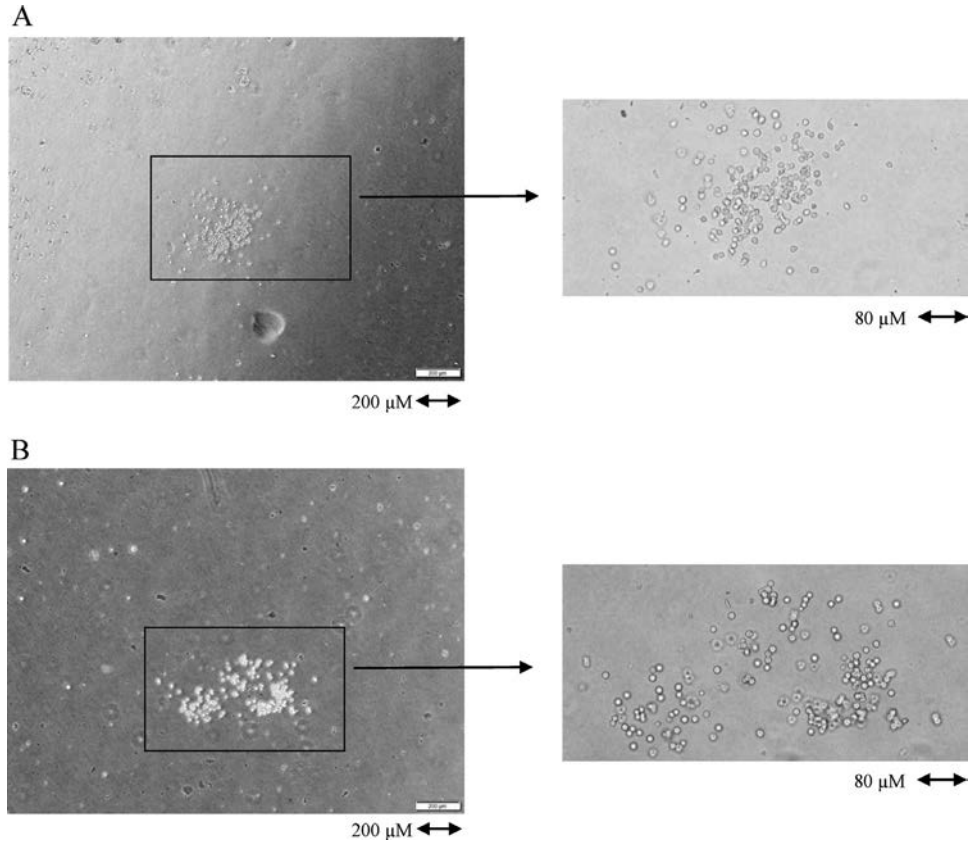

Figure 2. CD34$^+$CD38$^-$CD123$^+$ cells give rise to blast-like/monocytic colonies. Représentative images of a colony forming assay that was performed on sorted CD34$^+$CD38$^-$CD123$^+$ obtained from 2 AML patients: **A.** patient AML15. **B**. patient AML22. Images were taken using an inverted light microscope.

recognizing p65 or with normal mouse IgG (as a negative control), followed by standard protein immunoprecipitation. DNA–protein crosslinks were reversed by incubating at 65°C with 0.2M NaCl. The recovered DNA was used in a PCR reaction. PCR was performed with primers for the HIF-1α promoter flanking the NF-κB-binding site (−197/188bp) (forward: 5′-GAACAGAGAGCCCAGCAGAG-3′ and reverse: 5′-CCTGAGGTGGAGGCGGGTTC-3′) at 64°C annealing and 72°C extension for 32 cycles. This primer set spans from −536 to −137bp from the transcription start site. The HIF-1α control primer set was 5′-TGCTCATCAGTTGCCACTTC-3′ (forward) and 5′-AAAACATTGCGACCACCTTC-3′ (reverse). This primer set is located in the gene itself, 24937bp away from the transcription start site [22]. DNA samples (input) before immunoprecipitation, corresponding to 1% of chromatin samples, were PCR amplified as loading controls.

Intracellular ROS measurement

Intracellular ROS levels were determined by 2′,7′-dichlorodihydrofluorescein diacetate (H_2DCFDA) cellular ROS detection assay kit (Abcam, Cambridge, UK). Sorted AML and KG-1a cells were cultured in 24-well plates (5×10^5 cells/well) in the presence of deferasirox for 3 hours. The cells were then overlaid with 40μM H_2DCFDA diluted in IMDM to a final concentration of 20μM H2DCFDA and incubated for 30 minutes at 37°C and then analyzed. Detection of free thiol groups was performed using Monochlorobimane (mBCl) (Thermo-Fisher Scientific) staining. Sorted AML and KG-1a cells were exposed to deferasirox for 30 minutes followed by staining with 25μM mBCl diluted in IMDM for 15 minutes at room temperature. Mitochondrial ROS detection was determined using the MitoSOX^{TM} Red Mitochondrial Superoxide Indicator (Thermo-Fisher Scientific) according to protocol. Exposure to 1 and 10μM doxorubicin (DOX) (Selleckchem) for 18 hours was used as positive control. The analyses were performed on a Gallios flow cytometer and the data were processed by Kaluza software (Beckman Coulter).

Western blot analysis

Protein samples were separated on 4-20% Mini-PROTEAN precast gels (Bio-Rad, Hercules, CA, USA), the gels were transferred to a nitrocellulose Trance-Blot Turbo Transfer Pack membrane (Bio-Rad) and blotted with the antibodies detailed below. Non-specific

binding was avoided by blocking the nitrocellulose membrane with 3% skimmed milk in tris-buffered saline and Tween 20 (TBS-T) for 1 hour. Antibodies were diluted in TBS-T with 5% BSA or 5% nonfat dry milk. The following antibodies were used: α-caspase-3, rabbit polyclonal, 1:1000, (Cell Signaling, Danvers, MA USA); α-PARP, rabbit polyclonal, 1:1000, (Cell Signaling); α-HIF-1α, rabbit polyclonal, 1:1000 (Cell Signaling); α-NFkB (p65), rabbit polyclonal 1:1000 (Santa Cruz, Santa Cruz, CA, USA); α-Histon H4, rabbit polyclonal, 1:1000, (Abcam); α-tubulin, polyclonal 1:10000 (Sigma Aldrich) and IRDye 800CW/680RD secondary antibodies, 1:7500 (LI-COR, Lincoln, NE, USA). The membranes were incubated with the primary antibodies overnight at 4 °C and with the loading control antibody and secondary antibody for 1 hour at room temperature. The signals were detected using the Odyssey Imaging System (LI-COR).

Real-time PCR

RNA was isolated from the different KG-1a and from the different AML patient cell fractions using the RNeasy Plus Mini Kit (Qaigen, Hilden, Germany). RNA was reverse transcribed using the high capacity cDNA RT kit (Applied Biosystems, Foster City, CA, USA). Real-time PCR was then performed using the Eco Real-Time PCR (Illumina, San Diego, CA, USA) in a 20μl reaction containing 10ng RNA, 10μl TaqMan Fast Advanced master mix (Applied Biosystems), 1μl of target gene or GUSB RNA control primers and a FAM dye-labeled TaqMan probe (Applied Biosystems). Amplification conditions were: 50°C for 2 minutes, followed by 95°C for 10 minutes, then 40 cycles of 95°C for 15 seconds and 60°C for 1 minute. The ΔΔCt method was used to calculate relative expression levels.

Colony-forming assay

AML patients' $CD34^+CD38^-CD123^+$ cells were exposed to deferasirox and colony assay was performed. Representative enlarged images of the colonies are shown in Figure 2. The colonies are mostly abnormal and exhibit blast-like or monocytic features with the exception of several granulocyte/macrophage (CFU-GM) colonies.